THE JOURNAL OF BIOLOGICAL CHEMISTRY
Vol. 278, No. 50, Issue of December 12, pp. 49812–49818, 2003
Printed in U.S.A.

The Voltage-dependent Anion Channel Is the Target for a New Class of Inhibitors of the Mitochondrial Permeability Transition Pore*

Received for publication, May 7, 2003, and in revised form, August 20, 2003
Published, JBC Papers in Press, September 2, 2003, DOI 10.1074/jbc.M304748200

Andrea M. Cesura‡§, Emmanuel Pinard‡¶, Robert Schubenel‡, Valerie Goetschy‡, Arno Friedlein‖, Hanno Langen‖, Peter Polcic, Michael A. Forte**, Paolo Bernardi‡‡, and John A. Kemp‡§§**

*From the ‡Pharmaceutical Division, Drug Discovery Department and ‖Genomics Technologies, F. Hoffmann-La Roche Ltd., Grenzacherstrasse 124, CH-4070 Basel, Switzerland, the **Vollum Institute, Oregon Health and Sciences University, Portland, Oregon 97201, and the ‡‡Department of Biomedical Sciences, University of Padova, Viale G. Colombo 3, I-35121, Padova, Italy*

The relevance of the mitochondrial permeability transition pore (PTP) in Ca^{2+} homeostasis and cell death has gained wide attention. Yet, despite detailed functional characterization, the structure of this channel remains elusive. Here we report on a new class of inhibitors of the PTP and on the identification of their molecular target. The most potent among the compounds prepared, Ro 68-3400, inhibited PTP with a potency comparable to that of cyclosporin A. Since Ro 68-3400 has a reactive moiety capable of covalent modification of proteins, [^{3}H]Ro 68-3400 was used as an affinity label for the identification of its protein target. In intact mitochondria isolated from rodent brain and liver and in SH-SY5Y human neuroblastoma cells, [^{3}H]Ro 68-3400 predominantly labeled a protein of ~32 kDa. This protein was identified as the isoform 1 of the voltage-dependent anion channel (VDAC). Both functional and affinity labeling experiments indicated that VDAC might correspond to the site for the PTP inhibitor ubiquinone$_0$, whereas other known PTP modulators acted at distinct sites. While Ro 68-3400 represents a new useful tool for the study of the structure and function of VDAC and the PTP, the results obtained provide direct evidence that VDAC1 is a component of this mitochondrial pore.

The mitochondrial PTP[1] has been increasingly recognized as a major player in the mitochondrial pathways leading to cell death (1–5). The PTP is triggered by Ca^{2+} influx into mitochondria and is modulated by a variety of factors that include mediators of intracellular signaling (2, 6, 7). While it has been proposed that the PTP may provide mitochondria with a fast Ca^{2+} release channel, thereby contributing to intracellular Ca^{2+} homeostasis and signaling (2, 8, 9), persistent opening of the PTP precipitates a bioenergetic crisis with collapse of $\Delta\psi_m$, ATP depletion, and Ca^{2+} deregulation. The PTP may also be instrumental in the release of mitochondrial apoptogenic proteins, such as cytochrome *c*, in programmed cell death (10). Several pieces of evidence suggest that mitochondrial dysfunction, associated with deregulation of the PTP, may play an important role in injury following ischemia/reperfusion (3, 9, 11) and neuronal damage following an excitotoxic insult (12). The PTP inhibitor CsA has been found to delay/reduce glutamate-induced mitochondrial membrane depolarization and cell death (13, 14) and to be neuroprotective in animal models of ischemia and brain trauma (15–17). Since non-immunosuppressive CsA analogues, such as *N*-MeVal4-CsA, have also been shown to have neuroprotective properties (18), this indicates that CsA is likely to act specifically to antagonize PTP dysfunction in these *in vivo* models.

Despite detailed functional characterization, much of the information on the molecular nature of the PTP relies on indirect evidence and its precise molecular nature still remains elusive. The PTP is assumed to be due to the formation of dynamic multiprotein complexes at OMM and IMM contact sites (3, 5). These complexes are thought to involve the ANT in the IMM, in association with VDAC in the OMM, with a regulatory protein, Cyp-D, located in the matrix. Cyp-D is the target for CsA, and the only PTP regulatory protein identified so far with reasonable certainty (19). Several other proteins, including those of the Bcl-2 family, appear to participate in PTP regulation through poorly defined interactions (5).

CsA has become the standard pharmacological tool for the characterization of the PTP in isolated mitochondria, in living cells and *in vivo*. Other PTP inhibitors include ANT ligands such as ADP and BKA (1, 6), ubiquinone analogues (20–22), and a wide range of compounds, *e.g.* TFP and spermine, sharing the general property of being amphipathic cations (6, 23). However, the fact that the molecular target for most of the compounds reported to inhibit or induce PTP have not been directly identified, together with their poor specificity, has

* This work was supported by Grant R01-GM35759 from the National Institutes of Health (to P. P. and M. A. F.) and the MIUR (to P. B.). The costs of publication of this article were defrayed in part by the payment of page charges. This article must therefore be hereby marked "*advertisement*" in accordance with 18 U.S.C. Section 1734 solely to indicate this fact.

§ To whom correspondence may be addressed: Pharmaceutical Research and Development, Serono International S.A., Chemin des Aulx 12, CH-1228 Plan-les-Ouates, Switzerland. Tel.: 41-22-706-9465; Fax: 41-22-706-9550; E-mail: andrea.cesura@serono.com.

¶ To whom correspondence may be addressed: Pharmaceutical Division, Drug Discovery Department, 92/3.76, F. Hoffmann-La Roche Ltd, Grenzacherstrasse 124, CH-4070 Basel, Switzerland. Tel.: 41-61-688-4388; Fax: 41-61-688-8714; E-mail: emmanuel.pinard@roche.com.

§§ Present address: EVOTEC Neuroscience GmbH, 22525 Hamburg, Germany.

[1] The abbreviations used are: PTP, permeability transition pore; IMM, inner mitochondrial membrane; OMM, outer mitochondrial membrane; VDAC, voltage-dependent anion channel; Cyp-D, cyclophilin-D; ANT, adenine nucleotide translocase; $\Delta\psi_m$, mitochondrial membrane potential; CsA, cyclosporin A; Ub_0, ubiquinone 0; Ub_5, ubiquinone 5; FCCP, carbonyl cyanide *p*-trifluoromethoxyphenylhydrazone; BKA, bongkrekic acid; TFP, trifluoroperazine; TPP, tetraphenylphosphonium; ATR, atractyloside; DIDS, 4,4′-diisothiocyanatostilbene-2,2′-disulfonic acid; MALDI-MS, matrix-assisted laser desorption ionization-mass spectrometry; nanoESI-MS/MS, nanoelectrospray ionization tandem mass spectometry; MOPS, 4-morpholinepropanesulfonic acid.

hampered progress in elucidating PTP structure and pathophysiological relevance.

In this article, we report the identification of a new class of inhibitors of the PTP. We also took advantage of the fact that these compounds carry a reactive moiety to perform affinity-labeling experiments for identifying its binding protein on the PTP. These studies led to the identification of the isoform 1 of VDAC (VDAC1) as their molecular target, providing direct evidence that this protein is indeed a component of the PTP.

EXPERIMENTAL PROCEDURES

Compounds and Chemicals—Ro 04-2843 (6-bromo-3-diethylaminomethyl-chroman-4-one), Ro 68-3406 (6-bromo-3-methylene-chroman-4-one), Ro 68-3400 (spiro[cyclopentane-1,5′-[5H]dibenzo[*a,d*]cyclohepten]-2-one,10′,11′-dihydro-3-methylene) (see Fig. 1 for structures) were prepared at Hoffmann-La Roche Ltd, Basel, Switzerland. [^{3}H]Ro 68-3400 (65 Ci/mmol, 1 Ci = 37 Mbq) was kindly prepared by Dr. Thomas Hartung (Hoffmann-La Roche Ltd). [^{3}H]Tetraphenylphosphonium ([^{3}H]TPP, 24–29 Ci/mmol) was purchased from Amersham Biosciences (Switzerland). CsA, TFP, Ub_0, and Ub_5 were from Sigma; ATR and BKA from BioMol; Calcium-Green 5N, Rhodamine-123, and DIDS from Molecular Probes.

Preparation of Rat Liver Mitochondria—Liver and brain mitochondria were prepared from male Albino RoRo rats or MoRo mice (RCC, Basel, Switzerland). For swelling experiments, liver mitochondria were isolated by differential centrifugation according to standard procedures (21). Brain mitochondria were isolated from rat and mouse forebrain on a Percoll gradient as described in Ref. 24. For affinity labeling experiments also liver mitochondria were purified on a Percoll gradient.

Mitochondrial Swelling—Ca^{2+}-induced swelling in energized mitochondria was assayed at 25 °C in 96 well-plates by measuring changes in absorbance at 540 nm by means of a SPECTRAMax 250 spectrophometer controlled by the SOFTmax PRO™ software (Molecular Devices). The incubation medium contained 0.2 M sucrose, 10 mM Tris-MOPS, 1 mM P_i-Tris, 5 μM EGTA-Tris, pH 7.4. Succinate (5 mM, in the presence of 2 μM rotenone) or 5 mM glutamate and 2.5 mM malate, buffered to pH 7.4 with Tris, were used as respiratory substrates. After a ~5 min preincubation with or without test compounds, swelling was induced by the addition of 20 μl of $CaCl_2$ at final concentrations ranging from 40 to 80 μM. The final incubation volume was 0.2 ml and the concentration of mitochondria was ~0.5 mg mitochondrial protein/ml. Absorbance readings were taken every 12 s and the plate was shaken for 3 s between readings to ensure O_2 diffusion. Swelling experiments were also performed in fully de-energized liver mitochondria according to Ref. 25. EC_{50} values were determined from dose-response curves using at least 7 different inhibitor concentrations. Data, expressed as percentage changes in absorbance at 540 nm (ΔA540) *versus* baseline (no $CaCl_2$) 30 min after the addition of $CaCl_2$, were fitted to non-linear regression analysis using a four-parameter logistic equation using the SigmaPlot computer program.

[^{3}H]TPP Uptake and Oxygen Consumption—Isolated liver mitochondria (~0.5 mg protein/ml) were incubated in a batch mode in the presence of 20 nM [^{3}H]TPP for 15 min at 25 °C. Aliquots (100 μl) of the mixture were then distributed into 96-well plates containing 100 μl of the test compound and the incubation prolonged for 15 min at 25 °C. Samples were then filtered through 0.3% (v/v) polyethyleneimmine-treated GF/B glass fiber filters using a 96-channel cell harvester and the filters washed twice with 1 ml of buffer. 50 μl of MICROSCINT 40 (Packard) were then added to each well, before counting for radioactivity in a TopCount scintillation counter (Packard). Nonspecific uptake was determined in the presence of 1 mM unlabeled TPP or 1 μM FCCP. Oxygen consumption was determined polarographically using a Clark-type electrode

Measurement of Ca^{2+} Retention Capacity and of $\Delta\psi_m$ in Brain Mitochondria—Extramitochondrial Ca^{2+} was determined using a PerkinElmer LS-50B fluorimeter controlled by the FL WinLab computer program. The incubation medium contained 0.2 M sucrose, 1 mM P_i-Tris, 10 mM Tris-MOPS, 5 mM glutamate-Tris, 2.5 mM malate-Tris, pH 7.4, containing 0.01% (w/v) bovine serum albumin, and 1 μM of the Ca^{2+} indicator Calcium Green-5N (21). The final volume was 2.5 ml, and the cuvette was thermostatted at 25 °C. Brain mitochondria were subjected to a train of 5 μM Ca^{2+} additions and fluorescence monitored at excitation/emission wavelengths of 505–535 nm. Calibration of Ca^{2+} signals was performed according to the manufacturer's instructions assuming a K_D for the dye of 14 μM. For measurements of $\Delta\psi_m$, 0.5 μM rhodamine-123 was added instead of Calcium Green-5N and fluorescence monitored at 503–525 nm excitation/emission wavelengths (20).

Affinity Labeling of Mitochondria Using [^{3}H]Ro 68-3400—Percoll-purified mitochondria (~30 μg of protein per sample) were incubated for 15 min at 25 °C in the presence of 10 nM [^{3}H]Ro 68-3400 in a final volume of 200 μl. After rinsing, mitochondria were solubilized in sample buffer containing β-mercaptoethanol (1 h at 37 °C) and subjected to SDS-PAGE on Tris-glycine Novex precast gels (12% monomer concentration, Invitrogen). For fluorography, gels were soaked in Amplify™ (Amersham Biosciences), dried, and exposed at −80 °C to x-ray BioMax MS film with BioMax MS intensifying screen (Kodak).

Protein Purification and Identification—Mitochondria (~5 mg of proteins) were labeled as described above in the presence of 20 nM [^{3}H]Ro 68-3400 for 15 min at 25 °C, and solubilized with 3 ml of 3% Triton X-100 (Surfact-Amps X-100, Pierce) in 10 mM $NaPO_4$, pH 6.8, containing 0.5 mM phenylmethylsulfonyl fluoride, 1 μg/ml leupeptin, 1.8 μg/ml aprotinin, and 1 μg/ml pepstatin A (Roche Applied Science). Samples were then injected into a ceramic hydroxyapatite CHT-II 1 × 5 cm column (Bio-Rad) equilibrated in 10 mM $NaPO_4$, pH 6.8, containing 0.3% Triton X-100. The column was then eluted with $NaPO_4$ gradient, containing 0.3% Triton X-100, at a flow rate of 0.5 ml/min. Fractions (1 min) were collected and, an aliquot (5 μl) counted for radioactivity, and then subjected to SDS-PAGE, followed by staining and fluorography.

Proteins in the radioactive fractions were precipitated with trichloroacetic acid and, after carboxamidomethylation, submitted to SDS-PAGE. After staining with colloidal Coomassie Blue (Novex) and destaining, gel spots were excised and protein analyzed after in-gel digestion using modified trypsin (Promega) by MALDI-MS as previously described (26). Samples were analyzed in a time-of-flight PerSeptive Biosystems mass spectrometer equipped with a reflector. The peptide masses obtained were matched with the theoretical peptide masses of all proteins from all species in the SWISS-PROT and TrEMBL data base (us.expasy.org/sprot/). The identity of some of the tryptic fragments was also confirmed by nanoelectrospray ionization tandem MS (nanoESI-MS/MS) by means of an API 365 triple quadrupole mass spectrometer (Sciex) as previously described (27).

Yeast Methods—Saccharomyces cerevisiae yeast strains lacking the *Por1* gene (Δ*por1*) and containing plasmids mediating the expression of yeast (YVDAC1) and human VDAC1 (HVDAC1) were produced and mitochondria prepared as described (28–30). Affinity labeling experiments were performed in the presence of 10 nM [^{3}H]Ro 68-3400 as described above. A mouse monoclonal antibody directed against HVDAC1 [anti-porin 31HL (Ab-4), Calbiochem], and a rabbit polyclonal antibody against YVDAC1 (29) were used for VDAC detection by immunoblot in yeast mitochondrial preparations.

RESULTS

Screening and Identification of a New Class of PTP Inhibitors—In an effort to identify new inhibitors of the PTP, a compound library was screened using Ca^{2+}-induced swelling of rat liver mitochondria energized with succinate as a functional assay. Compounds found to inhibit swelling were then counter-screened using uptake of the potentiometic probe [^{3}H]TPP (31) to discard "false positives" (*e.g.* protonophores), which could have lowered the mitochondrial membrane potential and, thus, Ca^{2+}-influx into mitochondria. Compounds that did not interfere with mitochondrial respiration at the concentrations inhibiting the PTP were then selected for further characterization. Among these substances, our attention focused on a class of compounds inhibiting the PTP in the low micromolar range and having common pharmacophoric elements. These compounds were β-aminoketone derivatives, typically exemplified here by Ro 04-2843 (Fig. 1 and Table I). However, as also reported for a class molecules of close chemical structure (32), compounds with this structure are not stable at neutral pH, undergoing decomposition with $t_{1/2}$ of ~30 min at pH 7.4. The corresponding enone decomposition product of Ro 04-2843, *i.e.* Ro 68-3406 (Fig. 1), was, therefore, prepared and found to still inhibit PTP (Table I and Fig 2*B*). Preparation of a number of derivatives led then to the identification of a number of PTP inhibitors, including Ro 68-3400 (Fig. 1), which was identified as being the most potent.

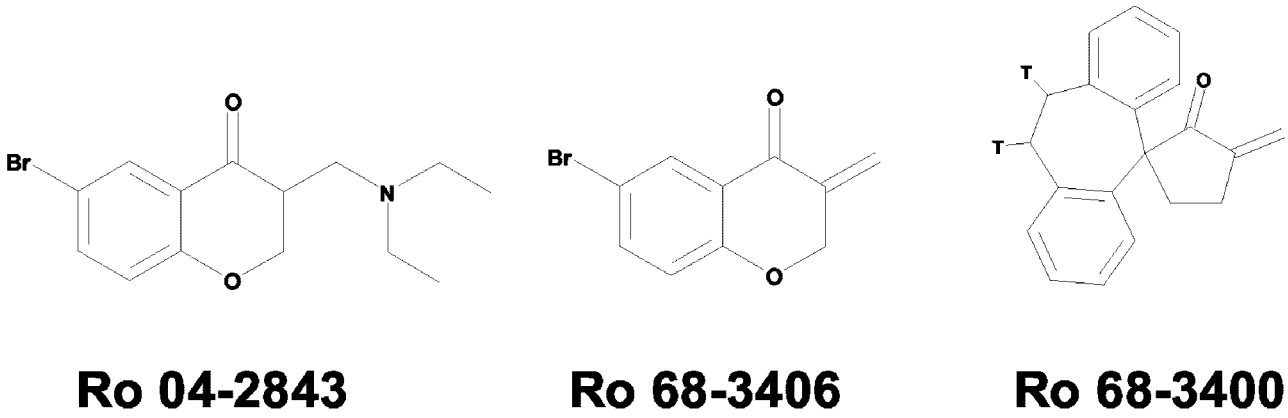

FIG. 1. **Chemical structure of Ro 04-2843, Ro 68-3406, and Ro 68-3400.** For Ro 68-3400, the positions of tritium (*T*) labeling are indicated.

TABLE I
Effect of various inhibitors on Ca^{2+}-induced PTP in rat liver mitochondria

The incubation medium consisted of 0.2 M sucrose, 1 mM P_i-Tris, 10 mM Tris-MOPS, pH 7.4. Succinate (5 mM, in the presence of 2 μM rotenone) was used as respiratory substrate. Swelling was induced by the addition of 80 μM Ca^{2+}. Values are mean ± S.E. The number of independent experiments performed for each compound is indicated is indicated in parentheses (*n*).

	EC_{50}	*n*
	μM	
Ro 04–2843	1.83 ± 0.39	(3)
Ro 68–3406	1.21 ± 0.43	(6)
Ro 68–3400	0.19 ± 0.03	(3)
CsA	0.30 ± 0.03	(4)
Ub_0	23.2 ± 2.3	(4)
ADP[a]	4.84 ± 0.73	(3)
BKA	11.5 ± 4.21	(4)
TFP	9.37 ± 3.32	(3)

[a] The experiments with ADP were performed in the presence of 1 μg/ml oligomycin.

Properties of Ro 68-3400 as PTP Inhibitor in Liver Mitochondria—The inhibition of Ca^{2+}-induced swelling in liver mitochondria energized with NADH-linked substrates (glutamate/malate) by Ro 68-3400 is shown in Fig. 2*A*. This compound inhibited PTP induced by addition of 40 μM Ca^{2+} with an EC_{50} of 98 ± 10 nM (Fig. 2*B*). Under similar conditions, CsA and Ro 68-3406 displayed EC_{50} values of 160 ± 9 and 930 ± 30 nM, respectively (Fig. 2*B*). Table I shows the EC_{50} obtained in succinate-energized mitochondria for Ro 68-3400 and related compounds in comparison to known PTP inhibitors. Ro 68-3400 was at least as effective as CsA at inhibiting PTP in liver mitochondria, and more potent than the other PTP inhibitors tested. While it has to be pointed out that the EC_{50} are relative values and depend on Ca^{2+} load as well as on respiratory substrates (see Ref. 20), the relative potencies of the various inhibitors were maintained at varying Ca^{2+} loads (data not shown).[2] Ro 68-3400 and Ro 68-3406 were also effective at inhibiting PTP in de-energized mitochondria, a condition where interaction with sites indirectly modulating PTP can be excluded (25, 33), with EC_{50} values of 0.37 and 2.8 μM, respectively (n = 2, 200 μM Ca^{2+}). For comparison, under these conditions, the EC_{50} values of CsA and Ub_0 were found to be 0.22 and 4.9 μM, respectively. At concentrations completely blocking PTP, Ro 68-3400 and Ro 68-3406 did not inhibit mitochondrial respiration (basal, ADP-induced and uncoupled), Ca^{2+} uptake by mitochondria or Cyp-D peptidyl prolyl *cis-trans* isomerase enzymatic activity (data not shown).

[2] A. M. Cesura, E. Pinard, R. Schubenel, N. Hauser, V. Goetschy, E. Milanesi, P. Bernardi, and J. A. Kemp, manuscript in preparation.

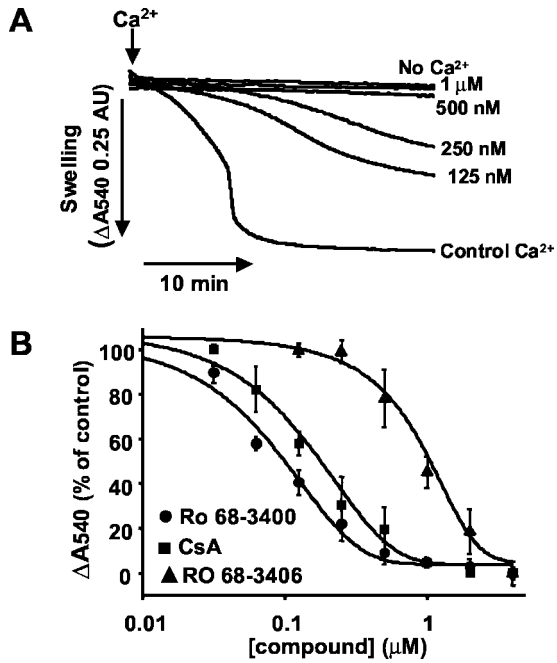

FIG. 2. **Inhibition of PTP by Ro 68-3400, Ro 68-3406, and CsA in liver mitochondria.** *A*, effect of Ro 68-3400 on Ca^{2+}-induced swelling in liver mitochondria energized with NADH-linked substrates (5 mM glutamate/2.5 mM malate). The incubation medium was 0.2 M sucrose, 1 mM P_i-Tris, 10 mM Tris-MOPS, 5 mM glutamate-Tris, 2.5 mM malate-Tris, pH 7.4. Mitochondrial swelling was induced by the addition of 40 μM $CaCl_2$ (*arrow*) and PTP opening monitored as the decrease in absorbance at 540 nm. The concentrations (nM) of Ro 68-3400 used in each trace are indicated. *B*, concentration-dependent inhibition of the PTP by Ro 68-3400 (●), Ro 68-3406 (▲), and CsA (■) in liver mitochondria. Experimental conditions were as above. Values shown are means ± S.E. from 3 to 5 experiments in duplicate using different liver mitochondrial preparations.

Effect of Ro 68-3400 on PTP in Brain Mitochondria—Ro 68-3400 inhibited swelling of brain mitochondria with a potency in the range of that observed for liver mitochondria (Fig. 3*A*). The effect of PTP inhibitors in brain mitochondria was also investigated by subjecting mitochondria to a series of 5 μM Ca^{2+} pulses and by monitoring extramitochondrial Ca^{2+} or $\Delta\psi_m$ using fluorescent probes (21). The effects of CsA and Ro 68-3400 in these experiments are shown in Fig. 3, *B* and *C*. Both Ro 68-3400 and CsA increased the ability of mitochondria to buffer Ca^{2+} until a threshold was reached at which no further Ca^{2+} could be taken up (Fig. 3*B*). At 1 μM (*i.e.* the maximal effective concentration observed for each inhibitor), both compounds approximately doubled the amount of Ca^{2+} taken up by brain mitochondria. Thus, control mitochondria

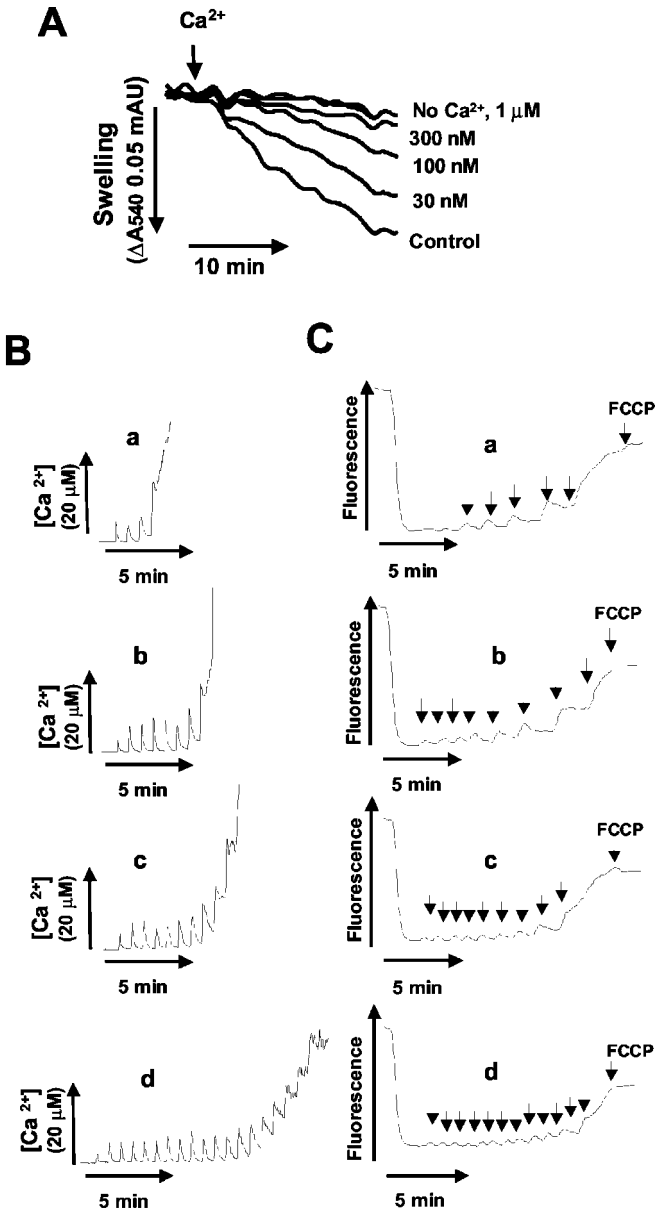

FIG. 3. **Inhibition of PTP by Ro 68-3400 and CsA in brain mitochondria.** *A*, effect of Ro 68-3400 on Ca^{2+}-induced swelling in brain mitochondria. Experimental conditions were as in Fig. 2, except that of 0.01% (w/v) bovine serum albumin was added to the medium, and swelling was induced by the addition of 80 μM $CaCl_2$. The concentrations of Ro 68-3400 used for each trace are indicated. *B*, determination of extramitochondrial Ca^{2+} after subsequent addition of 5 μM $CaCl_2$ pulses. The incubation medium consisted of 0.2 M sucrose, 1 mM P_i-Tris, 10 mM Tris-MOPS, 5 mM glutamate-Tris, 2.5 mM malate-Tris, pH 7.4, containing 0.01% (w/v) bovine serum albumin and 1 μM Calcium Green-5N. The final volume was 2.5 ml. *Traces* from *top* to *bottom* correspond to control (*a*), 1 μM CsA (*b*), 1 μM Ro 68-3400 (*c*), and 1 μM CsA plus 1 μM Ro 68-3400 (*d*). Each spike corresponds to addition of a Ca^{2+} pulse. *C*, determination of $\Delta\psi_m$ after subsequent addition of 5 μM Ca^{2+} pulses. Experimental conditions were as above except that 0.5 μM rhodamine-123 was used instead of Calcium Green-5N. *Arrows* indicate Ca^{2+} additions. The initial fluorescence quenching corresponds to addition of mitochondria. *Traces* from top to bottom are as in *panel B*.

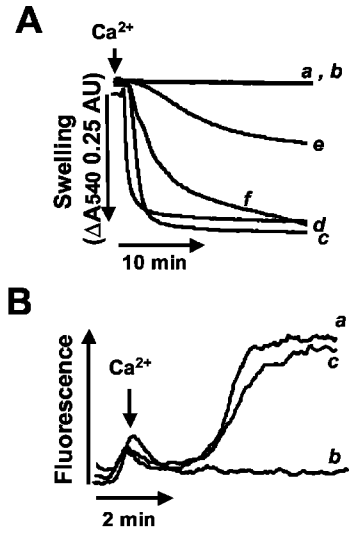

FIG. 4. **Ub_5 antagonizes the inhibition of PTP by Ro 68-3400.** *A*, effect of Ub_5 on inhibition of PTP by Ro 68-3400 in rat liver mitochondria. Experimental conditions were as in Fig. 2, except that 60 μM Ca^{2+} was added to induce the PTP. In *traces a* and *b* no Ca^{2+} was added with 50 μM Ub_5 present in *b*. For other traces, Ca^{2+} was added either alone, *trace c*, or in the presence of 50 μM Ub_5, *trace d*, 300 nM Ro 68-3400, *trace e*, and 300 nM Ro 68-3400 and 50 μM Ub_5, *f*. *B*, Ca^{2+}-induced depolarization of rat brain mitochondria. Experimental conditions were as in Fig. 3*C* except that a single pulse of 20 μM Ca^{2+} was added to induce mitochondrial depolarization. *Trace a*, control (Ca^{2+} alone), *trace b*, 300 nM Ro 68-3400, *trace c*, 300 nM Ro 68-3400 and 50 μM Ub_5.

were able to accumulate 530 ± 70 nmol of Ca^{2+}/mg of protein, whereas, in the presence of 1 μM CsA and Ro 68-3400, the Ca^{2+}-buffering capacity increased up to 1130 ± 80 and 1200 ± 120 nmol of Ca^{2+}/mg protein, respectively (mean ± S.E., $n = 3$). The combination of Ro 68-3400 and CsA had an additive effect, mitochondria being able to accumulate up to 2050 ± 450 nmol of Ca^{2+}/mg of protein. In agreement with the finding that Ro 68-3400 does not inhibit Cyp-D enzymatic activity, this indicates that Ro 68-3400 acts at a site in the PTP other than Cyp-D. Virtually identical results were obtained from experiments where $\Delta\psi_m$ was monitored after a series of Ca^{2+} additions (Fig. 3*C*). Each Ca^{2+} addition caused reversible decreases in $\Delta\psi_m$, until triggering of PTP completely collapsed $\Delta\psi_m$ and no further fluorescence increase could be observed after addition of the protonophore FCCP.

Similar experiments using other known PTP inhibitors also showed that the effect of Ro 68-3400 (and of Ro 68-3406) was additive with that of BKA, ADP, TFP, and tamoxifen, suggesting that Ro 68-3400 acts at a site that is different from those acted upon by these compounds (data not shown).[2] The only exception was Ub_0, a previously characterized PTP blocker (20) for which no such additive effect was seen.

Ro 68-3400 and Ubiquinone Derivatives—The lack of additive effect with Ub_0 suggested that the binding site of Ro 68-3400 might be related to the ubiquinone site reported to modulate the PTP (21, 22). To address this, we investigated whether Ub_5, an ubiquinone derivative able to relieve the inhibitory effect of Ub_0 (21), could similarly antagonize PTP inhibition by Ro 68-3400. As shown in Fig. 4*A* for rat liver mitochondria, Ub_5 (50 μM) was able antagonize the inhibition by Ro 68-3400, shifting its EC_{50} from 290 nM to 2.4 μM ($n = 2$). Likewise, in rat brain mitochondria, inhibition of Ca^{2+}-induced depolarization by 300 nM Ro 68-3400 was relieved by 50 μM Ub_5 (Fig. 4*B*).

Affinity Labeling of Mitochondria with [^{3}H]Ro 68-3400: Identification of VDAC1 as a Component of the Permeability Transition Pore—The high potency displayed by Ro 68-3400 at inhibiting the PTP and the fact it contains a reactive moiety, prompted us to tritiate the compound and use it as affinity labeling probe. Fig. 5*A* shows the results obtained after labeling with 10 nM [^{3}H]Ro 68-3400 of intact mitochondria isolated from rat brain and liver. A restricted number of proteins appeared to be labeled with a predominant band of ~32 kDa present in both preparations. A protein of identical size was

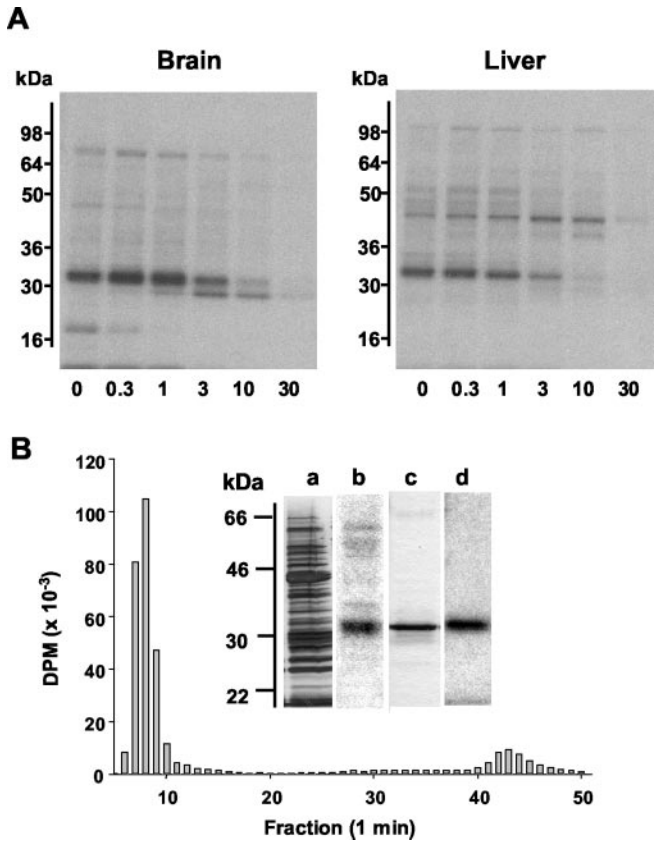

FIG. 5. **Affinity labeling of mitochondria by [^{3}H]Ro 68-3400 and purification of the 32-kDa labeled protein.** *A*, [^{3}H]Ro 68-3400 affinity-labeling of rat brain and liver mitochondria. Mitochondrial preparations were incubated in the presence of 10 nM [^{3}H]Ro 68-3400 for 15 min at 25 °C in the presence or absence of the indicated concentrations (μM) of unlabeled Ro 68-3400. The fluorograms of the SDS-PAGE gels are shown. The molecular mass scale (kDa) is shown in the ordinate. *B*, purification of the [^{3}H]Ro 68-3400 labeled 32 kDa protein. Triton X-100 solubilized rat liver mitochondria previously labeled with 20 nM [^{3}H]Ro 68-3400 were injected into a hydroxyapatite FPLC column. The column was eluted isocratically for 15 min and then with a linear gradient of $NaPO_4$, pH 6.8 (to 250 mM in 25 min, and then to 400 mM in 5 min). The histogram shows the radioactivity elution profile after counting an aliquot (5 μl) of the collected fractions. The *inset* shows the silver staining of Triton X-100 solubilized mitochondria (starting material, *lane a*) and of the column flow-through (fractions 7–9, *lane c*). The fluorograms of the corresponding starting and purified material are shown in *lanes b* and *d*, respectively.

also primarily labeled in mitochondria from mouse brain and liver, and from SH-SY5Y human neuroblastoma cells (not shown). Increasing concentration of unlabeled Ro 68-3400 inhibited radioactivity incorporation into this band. Notably, its labeling did not reflect a higher relative abundance, since Coomassie Blue and/or silver staining did not reveal major protein bands that correspond to the labeled protein (see *inset* to Fig. 5*B*).

This ~32 kDa protein labeled by [^{3}H]Ro 68-3400 in rat brain and liver mitochondria could be purified by a single FPLC chromatographic step using a hydroxyapatite column. As shown in Fig. 5*B*, most of the radioactivity eluted in the column front. SDS-PAGE analysis of these fractions, followed by silver staining and fluorography, showed the presence of a single radioactive protein (Fig. 5*B*, *inset*). MALDI-MS and nanoESI-MS/MS analysis revealed that the protein corresponded to the isoform 1 of VDAC (outer mitochondrial membrane protein porin 1, POR1_RAT, Q9Z2L0). VDAC1 was identified as the major protein labeled by [^{3}H]Ro 68-3400 also in mitochondria isolated from mouse brain and liver (POR1_MOUSE, Q60932) and SH-SY5Y cells (POR1_HUMAN, P21796). A protein with higher electrophoretic mobility became labeled in brain mitochondria in the presence of >1 μM Ro 68-3400 (Fig. 5*A*). Its identification by MALDI-MS in rat brain mitochondria labeled by [^{3}H]Ro 68-3400 in the presence of 3 μM Ro 68-3400, showed that it also corresponded to VDAC1. Thus, high Ro 68-3400 concentrations might alter VDAC1 electrophoretic mobility, possibly by reacting with more than one amino acid residue of the protein.

Two other proteins incorporating [^{3}H]Ro 68-3400 were also examined. The ~22-kDa band present in rat and mouse brain, but not in liver mitochondria and SH-SY5Y cells, was identified by nanoESI-MS/MS as BM88 (BM88_MOUSE, Q9JKC6), a neuron-specific protein involved in neuronal differentiation (34) found to be associated with the membrane of intracellular organelles including the limiting membrane of mitochondria (35). Although labeling of BM88 was inhibited by low concentration of Ro 68-3400 (Fig. 5*A*), due to its specific neuronal location, this protein does not appear to be a candidate as general PTP constituent and was not further considered in the present work. The ~45 kDa protein appearing only in mitochondrial preparations from liver and whose labeling was inhibited by high concentration of Ro 68-3400 (Fig. 5*A*) was identified as actin by immunoblot analysis using an anti-actin monoclonal antibody (Clone AC-40, Sigma) (data not shown).

To correlate the labeling of VDAC1 by [^{3}H]Ro 68-3400 with PTP inhibition, we tested the effect of a number of PTP inhibitors and of the PTP inducer ATR on the labeling of VDAC1 by [^{3}H]Ro 68-3400 in rat brain mitochondria. Incorporation of [^{3}H]Ro 68-3400 into VDAC1 was inhibited by its analogue Ro 68-3406 (as well as by Ro 04-2843, not shown) and by Ub_0 concentrations that block the PTP. Unexpectedly, however, Ub_5 did not affect radioactivity incorporation (Fig. 6*A*). Incorporation of [^{3}H]Ro 68-3400 into VDAC1 was also inhibited by DIDS, an anion channel blocker (36) which has been shown to inhibit superoxide-induced VDAC-dependent cytochrome *c* release from mitochondria (37). CsA, ADP, BKA, ATR, and TFP had no effect (Fig. 6*A*). Virtually identical results were obtained using rat liver mitochondria (data not shown).

[^{3}H]Ro 68-3400 Labeling in Yeast Mitochondria—We next investigated the labeling of yeast mitochondrial proteins by [^{3}H]Ro 68-3400. Virtually no labeling was detected in mitochondria from strains lacking the major VDAC isoform, YVDAC1, after deletion of the *Por1* (Δ*por1*) gene (Fig. 6*B*). After plasmid-mediated expression of YVDAC1 in Δ*por1* strains we observed the prominent labeling of a 29 kDa protein, the expected size of YVDAC (Fig. 6*C*, *lane b*). Increasing concentrations of unlabeled Ro 68-3400 inhibited incorporation of the radioactivity (Fig. 6*B*). Surprisingly, however, no labeling was detected when HVDAC1 rather than YVDAC1 was expressed in the Δ*por1* strains despite the fact that both proteins were expressed and targeted to mitochondria (Fig. 6*C*). Preliminary experiments also showed that no [^{3}H]Ro 68-3400 labeling was observed at the expected molecular masses after transfection of Δ*por1* strains with YDAC2, HVDAC2, and HVDAC3 (data not shown).

DISCUSSION

The results reported in the present study describe the identification and characterization of a new class of inhibitors of the PTP. The most potent compound obtained so far, Ro 68-3400, inhibited PTP with potency comparable to that of CsA. Moreover, affinity labeling experiments using [^{3}H]Ro 68-3400 identified VDAC1 as a major molecular target of Ro 68-3400 in mitochondria prepared from rodent brain and liver, and from a human neuroblastoma cell line. Finally, the results obtained support the notion that Ro 68-3400 and Ub_0 may act at the same and/or functionally related sites in the PTP.

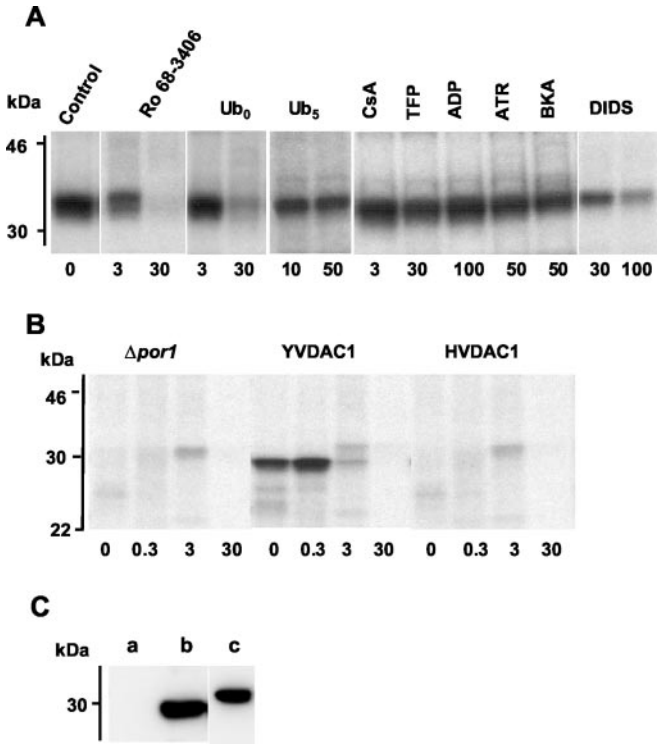

FIG. 6. **Labeling of VDAC1 by [^{3}H]Ro 68-3400 in brain mitochondria in the presence of various compounds and in *δpor1* yeast mitochondria transfected with yeast and human VDAC1.** *A*, effect of various PTP inhibitors, Ub_5, ATR, and DIDS on VDAC1 labeling by 10 nM [^{3}H]Ro 68-3400 in rat brain mitochondria. Experimental conditions were as in the legend to Fig. 5*A*. The compounds at the indicated concentrations (μM) were added together with [^{3}H]Ro 68-3400, except for DIDS, for which, in order to remove the reagent, mitochondria were exposed DIDS for 5 min, followed by centrifugation, rinsing, and resuspension before labeling with [^{3}H]Ro 68-3400. *B*, [^{3}H]Ro 68-3400 affinity labeling of yeast mitochondria lacking the *Por1* gene for YVDAC1 (Δ*por1*) and of Δ*por1* yeast mitochondria transfected with YVDAC1 and HVDAC1. Mitochondria isolated from yeast strains were incubated in the presence of 10 nM [^{3}H]Ro 68-3400 in the presence of the indicated concentration of unlabeled Ro 68-3400 (μM). The fluorograms of gels after SDS-PAGE are shown. *C*, immunoblot analysis of yeast and human VDAC expressed in Δ*por1* yeast strains. *Lane a*, Δ*por1*; *lane b*, *YDAC1*; *lane c*, *HVDAC*.

As mentioned in the Introduction, the precise structure and function of the PTP is still a matter of controversy. VDAC, together with ANT, were the first proteins proposed to constitute the PTP, initially on the basis of mostly theoretical arguments (1). More recently, experimental evidence has added weight to this proposition and VDAC has gained increasing attention as a possible PTP constituent (38, 39) and as a key protein controlling Ca^{2+} homeostasis by mitochondria (40). Here, we show that compounds like Ro 68-3400 that bind to VDAC1 behave as potent PTP inhibitors, providing direct evidence that VDAC1 is a component of this mitochondrial pore. The possibility that other proteins less intensely labeled by [^{3}H]Ro 68-3400 may represent additional PTP constituents cannot be entirely ruled out at present. Yet, the fact that VDAC1 was the only protein predominantly labeled in a consistent manner in all mitochondrial preparations strongly indicates that this protein represents the main target for Ro 68-3400. Independent evidence that VDAC1 is a component of the PTP comes from the fact that Ub_0, a structurally unrelated inhibitor, prevented incorporation of radioactivity into VDAC1 at concentrations inhibiting the PTP. While Ub_5 was able to functionally compete with Ro 68-3400 and Ub_0 (21) for PTP inhibition, it did not prevent VDAC1 labeling by [^{3}H]Ro 68-3400. We therefore suspect that the complex effects of quinones on the PTP (20–22) may depend on interactions at more than one site, an issue that deserves further study.

While clearly implicating VDAC in the PTP, several questions remain. First, it is still not clear why only VDAC1, among the expressed isoforms, was identified as the target protein for Ro 68-3400. Ro 68-3400 might react with specific nucleophilic amino acid(s) in VDAC1 that are not accessible in the other isoforms. Alternatively, VDAC1 may represent the predominant form expressed in the tissues tested (41). On the other hand, both VDAC1 and VDAC2 are ubiquitously expressed, while VDAC3 has a more restricted organ distribution (42–44). VDAC isoforms appear to display different physiological functions (45), each isoform exhibiting different permeability properties (46), and binding of hexokinase, a protein that has also been proposed to be associated to the PTP (47, 48), appears to be a specific feature of VDAC1 (28). It might, thus, be conceivable that only VDAC1 preferentially or exclusively takes part in PTP formation through specific interactions with partner protein(s) in the IMM. Experiments using mitochondria isolated from mice in which the gene encoding VDAC1 has been knocked out (49) will be instrumental to assess if Ro 68-3400 can also modify mammalian VDAC2 and 3.

The mechanistic basis of the inhibitory effect of Ro 68-3400 on the PTP also remains to be elucidated. Experiments not reported here and performed using Ro 68-3400 analogues lacking the reactive group, clearly showed that covalent modification of amino acid residue(s) is essential for conferring the high potency of Ro 68-3400 at inhibiting the PTP. Although technical difficulties have so far hindered the identification of the amino acid(s) modified by Ro 68-3400, further effort aimed at the identification of these residue(s) will be valuable for identifying critical VDAC1 domains possibly responsible for PTP gating (50) or involved in the dynamics of VDAC1 assembly with other PTP components. Interestingly, it was found that Ro 68-3400 and Ro 68-3406 failed to alter the electrophysiophysiological properties of VDAC channels incorporated into lipid bilayers (data not shown). As this was the case also for Ub_0, which inhibits the "mitochondrial megachannel" corresponding to the PTP (51), inhibition of PTP by these compounds cannot simply be ascribed to changes in permeability of VDAC itself, but would be more likely mediated through binding to a particular VDAC conformation shaped by its association with other proteins participating in the PTP.

The finding that [^{3}H]Ro 68-3400 specifically labels YVDAC1, but not HVDAC1, after transfection in Δ*por1* yeast strains, represents an unexpected but interesting finding. If the VDAC1 conformation recognized by Ro 68-3400 in mammalian mitochondria depends on a structure that is present only in association with other proteins, YVDAC1 might form productive association with partner yeast protein(s) which are required for recognition by this compound for PTP occurrence in yeast (52), whereas HVDAC1, due to the low sequence similarity with its yeast homologue, would not be able to assume such conformation in the context of yeast mitochondria. These findings are consistent with the hypothesis that only a specific conformation assumed by VDAC1 associated with PTP partner protein(s) would be able to bind Ro 68-3400 in intact mitochondria.

Definition of the detailed mechanism of PTP inhibition by Ro 68-3400 and of its interactions with the quinone binding site(s), together with identification of the structural requirements for VDAC1 binding and of the modified amino acid residue(s) are under active investigation. However, the identification of a novel class of PTP inhibitors and of their molecular target appears to be a critical step toward the molecular definition of the PTP and the development of novel mitochondrial drugs.

Acknowledgments—We express thanks to Dr. Thomas Hartung for preparation of [^{3}H]Ro 68-3400, Daniel Roeder (Hoffmann-La Roche Ltd., Basel) for assistance in protein analysis, and to Prof. Mario Zoratti, (CNR Institute of Neurosciences, Padova, Italy) for electrophysiological experiments of VDAC incorporated into lipid bilayers.

REFERENCES

1. Zoratti, M and Szabò, I. (1995) *Biochim. Biophys. Acta* **1241,** 139–176
2. Bernardi, P. (1999) *Physiol. Rev.* **79,** 1127–79155
3. Crompton, M. (1999) *Biochem. J.* **341,** 233–249
4. Bernardi, P., Petronilli, V., Di Lisa, F., and Forte, M. (2001) *Trends Biochem. Sci.* **26,** 112–117
5. Zamzami, N., and Kroemer, G. (2001)) *Nat. Rev. Mol. Cell. Biol.* **2,** 67–71
6. Gunter, T. E., Gunter, K. K., Sheu, S.-S., and Gavin, C. E. (1994) *Am. J. Physiol.* **267,** C313-C339
7. Scorrano, L., Penzo, D., Petronilli, V., Pagano, F., and Bernardi, P. (2001) *J. Biol. Chem.* **276,** 12035–12040
8. Ichas, F., Jouaville, L. S., and Mazat, J. P. (1997) *Cell* **89,** 1145–1153
9. Duchen, M. R. (2000) *J. Physiol.* **529,** 57–68
10. Newmeyer, D. D., and Ferguson-Miller, S. (2003) *Cell* **112,** 481–490
11. Di Lisa, F., Menabo, R., Canton, M., Barile, M., and Bernardi, P. (2001) *J. Biol. Chem.* **276,** 2571–2575
12. Nicholls, D. G., and Budd, S. L. (2000) *Physiol. Rev.* **80,** 315–360
13. Schinder, A. F., Olson, E. C., Spitzer, N. C., and Montal, M. (1996) *J. Neurosci.* **16,** 6125–6133
14. Vergun, O., Keelan, J., Khodorov, B. I., and Duchen, M. R. (1999) *J. Physiol.* **519,** 451–466
15. Friberg, H., Ferrand-Drake, M., Bengtsson, F., Halestrap, A. P., and Wieloch, T. (1998) *J. Neurosci.* **18,** 5151–5159
16. Yoshimoto, T., and Siesjo, B. K. (1999) *Brain. Res.* **839,** 283–291
17. Okonkwo, D. O., and Povlishock, J. T. (1999) *J. Cereb. Blood Flow Metab.* **19,** 443–451
18. Khaspekov, L., Friberg, H., Halestrap, A., Viktorov, I., and Wieloch T. (1999) *Eur. J. Neurosci.* **11,** 3194–3198
19. Nicolli, A., Basso, E., Petronilli, V., Wenger, R. M., and Bernardi, P. (1996) *J. Biol. Chem.* **271,** 2185–2192
20. Fontaine, E., Ichas, F., Bernardi, P. (1998) *J. Biol. Chem.* **273,** 25734–25740
21. Fontaine, E., Eriksson, O., Ichas, F., and Bernardi, P. (1998) *J. Biol. Chem.* **273,** 12662–12668
22. Walter, L., Nogueira, V., Leverve, X., Heitz, M. P., Bernardi, P., and Fontaine, E. (2000) *J. Biol. Chem.* **275,** 29521–29527
23. Broekemeier, K. M., and Pfeiffer, D. R. (1995) *Biochemistry* **34,** 16440–16449
24. Sims, N. R. (1990) *J. Neurochem.* **55,** 698–707
25. Chernyak, B. V., and Bernardi, P. (1996) *Eur. J. Biochem.* **238,** 623–630
26. Fountoulakis, M., and Langen, H. (1997) *Anal. Biochem.* **250,** 153–156
27. Krapfenbauer, K., Berger, M., Friedlein, A., Lubec, G., and Fountoulakis, M. (2001) *Eur. J. Biochem.* **268,** 3532–3537
28. Blachly-Dyson, E., Zambronicz, E., Yu, W-H., Adams, V., McCabe, E., Adelman, J., Colombini, M., and Forte, M. (1993) *J. Biol. Chem.* **268,** 1835–1841
29. Blachly-Dyson, E., Song, J., Wolfgang, W. J., Colombini, M., and Forte, M. (1997) *Mol. Cell. Biol.* **17,** 5727–5738
30. Gross, A., Pilcher, K., Blachly-Dyson, E., Basso, E., Jockel, J., Bassik, M. C., Korsmeyer, S. J., and Forte, M. (2000) *Mol. Cell. Biol.* **20,** 3125–3136
31. Hoek, J. B., Nicholls, D. G., and Williamson, J. R. (1980) *J. Biol. Chem.* **255,** 1458–1564
32. Ward, E. F., Garling, D. L., Buckler, R. T., Lawler, D. M., and Cummings, D. P. (1981) *J. Med. Chem.* **24,** 1073–1077
33. Linder, M. D., Morkunaite-Haimi, S., Kinnunen, P. K., Bernardi, P., and Eriksson, O. (2002) *J. Biol. Chem.* **277,** 937–942
34. Mamalaki, A., Boutou, E., Hurel, C., Patsavoudi, E., Tzartos, S., and Matsas, R. (1995) *J. Biol. Chem.* **270,** 14201–14208
35. Patsavoudi, E., Merkouri, E., Thomaidou, D., Sandillon, F., Alonso, G., and Matsas, R. (1995) *J. Neurosci. Res.* **40,** 506–518
36. Liu, G., Hinch, B., Davatol-Hag, H., Lu, Y., Powers, M., and Beavis, A. D. (1996) *J. Biol. Chem.* **271,** 19717–19723
37. Madesh, M., and Hajnoczky, G. (2001) *J. Cell Biol.* **155,** 1003–1015
38. Crompton, M., Virji, S., and Ward, J. M. (1998) *Eur. J. Biochem.* **258,** 729–735
39. Shimizu, S., Narita, M., and Tsujimoto, Y. (1999) *Nature* **399,** 483–487
40. Rapizzi, E., Pinton, P., Szabadkai, G., Wieckowski, M. R., Vandecasteele, G., Baird, G., Tuft, R. A., Fogarty, K. E., and Rizzuto, R. (2002) *J. Cell Biol.* **159,** 613–624
41. Huzing, M., Ruitenbeek, W., van dem Heuvel, P., Dolce, V., Iacobazzi, V., Smeitink, J. A. M., Palmieri, F., and Trijbels, J. M. F. (1998) *J. Bioenerg. Biomembr.* **30,** 277–284
42. Yu, W-H., Wolfgang, W., and Forte, M. (1995) *J. Biol. Chem.* **270,** 13998–14006
43. Sampson, M. J., Lovell, R. S., and Craigen, W. J. (1997) *J. Biol. Chem.* **272,** 18966–18973
44. Shinohara, Y., Ishida, T., Hino, M., Yamazaki, N., Baba, Y., and Terada, H. (2000) *Eur. J. Biochem.* **267,** 6067–6073
45. Cheng, E. H., Sheiko, T. V., Fisher, J. K., Craigen, W. J., and Korsmeyer, S. J. (2003) *Science* **301,** 513–517
46. Xu, X., Decker, W., Sampson, M. J., Graigen, W., and Colombini, M. (1999) *J. Membr. Biol.* **170,** 89–102
47. Beutner, G., Ruck, A., Riede, B., Welte, W., and Brdiczka, D. (1996) *FEBS Lett.* **396,** 189–195
48. Pastorino, J. G., Shulga, N., and Hoek, J. B. (2002) *J. Biol. Chem.* **277,** 7610–7618
49. Anflous, K., Armstrong, D. D., and Craigen, W. J. (2001) *J. Biol. Chem.* **276,** 1954–1960
50. Song, J., Midson, C., Blachly-Dyson, E., Forte, M., and Colombini, M. (1998) *Biophys. J.* **74,** 2926–2944
51. Martinucci, S., Szabò, I., Tómbola, F., and Zoratti, M. (2000) *FEBS Lett.* **480,** 89–94
52. Jung, D. W., Bradshaw, P. C., and Pfeiffer, D. R. (1997) *J. Biol. Chem.* **272,** 21104–21112

The Voltage-dependent Anion Channel Is the Target for a New Class of Inhibitors of the Mitochondrial Permeability Transition Pore

Andrea M. Cesura, Emmanuel Pinard, Robert Schubenel, Valerie Goetschy, Arno Friedlein, Hanno Langen, Peter Polcic, Michael A. Forte, Paolo Bernardi and John A. Kemp

J. Biol. Chem. 2003, 278:49812-49818.
doi: 10.1074/jbc.M304748200 originally published online September 2, 2003
